Available online at www.sciencedirect.com

SciVerse ScienceDirect

Ceramics International 39 (2013) 7551–7556

CERAMICS INTERNATIONAL

www.elsevier.com/locate/ceramint

Effect of the addition of polyvinylpyrrolidone as a pore-former on microstructure and mechanical strength of porous alumina ceramics

Yi Feng[a], Kun Wang[a], Jianfeng Yao[a], Paul A. Webley[a,b], Simon Smart[c], Huanting Wang[a,*]

[a]*Department of Chemical Engineering, Monash University, Clayton, Victoria 3800, Australia*
[b]*Department of Chemical and Biomolecular Engineering, The University of Melbourne, Melbourne, Victoria 3010, Australia*
[c]*FIMLab – Films and Inorganic Membrane Laboratory, School of Chemical Engineering, The University of Queensland, Brisbane, QLD 4072, Australia*

Received 1 January 2013; received in revised form 17 February 2013; accepted 2 March 2013
Available online 14 March 2013

Abstract

The effect of the solvent on the properties of porous alumina ceramics was studied when polyvinylpyrrolidone (PVP) was used as an organic pore-former. In particular, porous alumina ceramics were produced by dry-pressing of mixed PVP–alumina powder; the mixing of PVP and alumina powder was achieved via ball milling using water or acetone as solvent, or dry ball milling. Due to the different solubility of PVP in water and acetone, porous alumina ceramics with different pore structures and mechanical properties were obtained. Because of its cylindrical pores being aligned to some extent, the sample prepared using acetone as solvent exhibited the highest bending strength (140.2 MPa) and Young's modulus (57.4 GPa), which were 1.6 times and 3.4 times higher compared to that prepared without PVP. Moreover, the addition of PVP via wet ball milling led to more uniform dispersion of PVP in alumina, hence limiting the grain growth during sintering process and increasing the grain bonding.

Keywords: Mechanical properties; Porous ceramics; PVP; Microstructure

1. Introduction

Materials containing tailored porosity exhibit special properties and features that usually cannot be achieved by their conventional dense counterparts. Therefore, porous materials find numerous applications as end products and in several technological processes. Contrary to porous polymers, porous ceramics are more inert to various chemicals, bacteria and harsh environment such as high temperature and high pressure, and they are widely used as filters, catalyst supports, electrodes for solid oxide fuel cells and chemical or electronic sensors [1–3]. However, the brittleness of porous ceramics is the main concern for those applications requiring very good mechanical properties, such as ceramic hollow membranes. Especially, as separation membranes, a high porosity is needed to minimize the permeation resistance, and this leads to a decrease in the toughness of ceramic membranes. It still remains a challenge to retain the mechanical strength while a large volume of pores is introduced into the ceramic structures[4]. Therefore, there is a need for developing an effective way to prepare porous ceramics with excellent mechanical properties for industrial use.

There are numerous methods for increasing porosity of ceramics, such as by partial sintering or selection of a granular composition for initial molding mixture [5,6]; introduction of additives (PMMA, PVA, starch, $Al(OH)_3$, etc.) and their subsequent removal by evaporation, dissolution, burning-out or decomposition [7–10]; involvement of air into ceramic suspension or gas bubbles arising from chemical reaction or decomposition of pore-former [11]; extrusion of plasticized ceramic mixtures [12]. Porous ceramic materials are usually made by several shape-forming processes such as dry-pressing, isopressing, slip-casting, freeze-casting and so on. The simple dry-pressing method was used in the present work to study how the additive affects the properties of porous alumina ceramics.

Polyvinylpyrrolidone (PVP) is a water-soluble polymer and is usually used as an additive in the fabrication of ceramic

*Corresponding author. Tel.: +61 3 9905 3449.
E-mail address: huanting.wang@monash.edu (H. Wang).

0272-8842/$ - see front matter © 2013 Elsevier Ltd and Techna Group S.r.l. All rights reserved.
http://dx.doi.org/10.1016/j.ceramint.2013.03.007

membranes [13,14]. However, there are few studies on the relationship between different pore structures and mechanical properties of porous ceramics prepared using different solvents in dissolving and mixing the pore-former PVP and ceramic powder. As a water-soluble polymer, PVP can be readily dissolved in polar solvents such as NMP and ethanol while it has a limited solubility in non-polar solvents such as acetone. The solubility difference in different solvents can lead to different PVP particle sizes, which is expected to affect the pore morphology in the final porous ceramic materials and thus their mechanical properties. In this study, water and acetone were used as solvents to prepare mixed PVP–alumina powders for formation of porous alumina ceramics by the dry pressing method, in comparison with direct use of the raw PVP powder. The pore morphology and mechanical properties of the final porous ceramics were characterized and compared, with the goal of improving our understanding of how the procedure for addition of PVP affects the microstructure and mechanical structure of porous alumina ceramics.

2. Experimental

2.1. Preparation of porous ceramics

15 g of acetone (purity≥99.0%, Merck Schuchardt OHG) or deionized water were used to dissolve 1.5 g of PVP (average molecular weight 40,000, Sigma-Aldrich), respectively, followed by adding 15 g of alumina powder (d_{50}=1.2 μm, PP5010, Shell-lap Supplies Pty Ltd) and ball milling. The weight ratio of solvent and alumina was 1:1. After ball-milling for 48 h, the powder was dried and ground with a mortar and pestle. For comparison, dry ball-milling of PVP–alumina powder was carried out. The methods for preparing PVP–alumina powders were referred to as Method A, Method W, and Method D (dry milling) for the use of acetone, water and dry milling respectively. The PVP–alumina powder was uniaxially pressed into rectangular bars with the size of 50.9 mm×5.9 mm×3.0 mm at a pressure of 20 MPa. The porous alumina bars were then obtained by sintering the green compacts using a heating profile as follows: 600 °C for 1 h, to 1000 °C for 1 h and then to 1500 °C for 10 h at a heating rate of 3 °C/min. Samples are indicated as *X*–*Y*, while *X* refers to the method used, *Y* refers to the quantity (in percentage) of PVP added, e.g. A-10 means acetone was used to prepare 10 wt% PVP/alumina powder.

2.2. Characterization

The mean particle size of PVP in water and acetone was determined using a Mastersizer 2000 (Malvern instruments Ltd, UK). The porosities of the samples were measured using the Archimedes' method with deionized water as a liquid medium. The pore size distribution of the samples was measured by mercury porosimetry (Auto pore III mercury porosimeter, Particle and Surface Sciences Pty. Ltd. USA).The morphology and pore structures of the porous alumina were observed by scanning electron microscopy (Nova Nano SEM, FEI company), and the average grain size of sintered samples was measured by the linear intercept technique based on SEM images [15]. The linear sintering shrinkage of the samples was determined by measuring the length of the samples before and after sintering.

The mechanical strength was determined by the three-point bending test (Mini-instron) with a span of 20 mm and a crosshead speed of 0.5 mm/min. For each batch, at least five specimens were tested and the average strength was calculated and the standard deviation *s* was also calculated to show the variability of the tested samples.

3. Results and discussion

3.1. Dissolution of PVP in different solvents

PVP is slightly dissolved in acetone, and well dissolved in water. The mean PVP particle size in acetone was determined to be 5.26 μm while its mean particle size was only 39 nm in water. From the SEM images of raw samples shown in Fig. 1, it can be seen that individual particles are clearly observed in A-10 compact while the particles are floccule-like in W-10 compact, indicating PVP is better dispersed in W-10 than A-10. This can be attributed to different particle sizes of PVP in the preparation of PVP–alumina mixtures, i.e., PVP nanoparticles were uniformly dispersed and well bound with alumina particles.

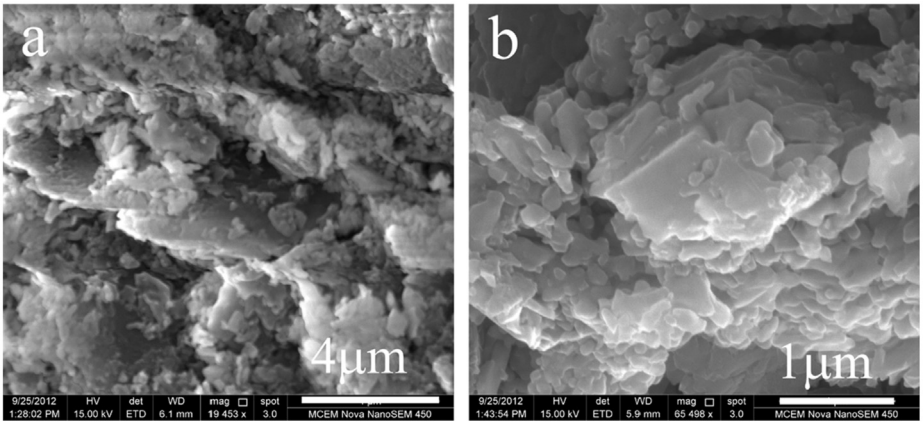

Fig. 1. SEM images of compact samples: (a) W-10 and (b) A-10.

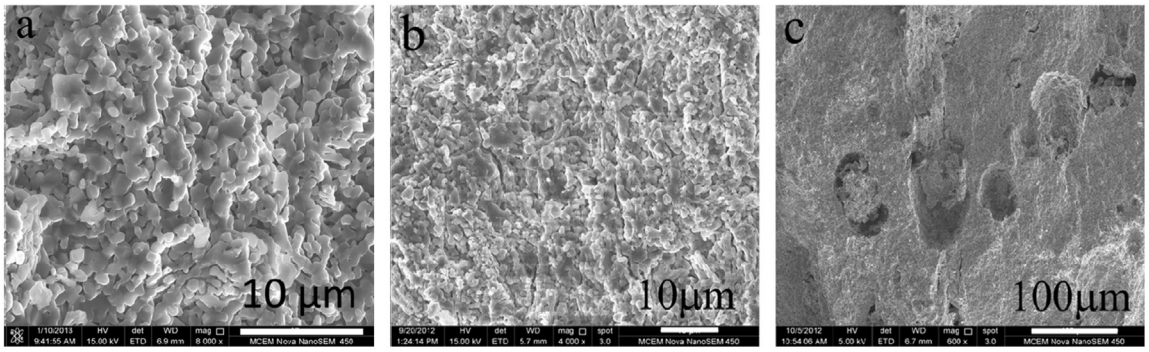

Fig. 2. SEM images of cross sections of sintered samples: (a) W-10, (b) A-10 and (c) D-10 sample.

Table 1
Linear shrinkage and porosity of sintered samples.

Sample	A-0	A-5	A-10	A-20	W-10	D-10
Linear shrinkage (%)	14.6	13.7	13.7	12.8	15.4	14.7
Porosity (%)	32.0	33.8	31.3	40.9	30.2	43.5

3.2. Microstructure

Fig. 2 shows the SEM images of sintered porous alumina ceramics prepared via different methods. Sample W-10 exhibits more uniform pore structure than A-10 and D-10. In A-10, many pores appear to be connected together, forming long and narrow porous channels while a significant number of large pores with a few tens of microns in size can be observed in D-10 sample and are created by decomposition of large PVP particles. Unlike wet ball-milling, dry ball-milling could only mix raw PVP and alumina powder and likely reduced PVP particle sizes slightly. Therefore, large PVP particles with wide size distribution existed in the compacts after shaping, leading to large pores after PVP burn-off in the sintering process.

3.3. Porosity and pore size distribution

The porosity of all samples is in the range of 30%–45% as shown in Table 1. Comparing different powder-mixing methods, sample D-10 prepared via dry mixing has the highest porosity (43.5%), while samples W-10 and A-10 have a similar porosity of around 30%. Fig. 3 shows the pore size distribution of samples made using different mixing methods. It can be seen that sample D-10 has some large pores and a wide pore size distribution. This is supported by SEM results. The pore size distributions for samples A-10 and W-10 did not show much difference except that the mean pore size of sample W-10 (0.2 μm) is slightly smaller than that of sample A-10 (0.3 μm). It is noted that the pore size distribution determined by mercury porosimetry does not reflect the difference in the pore shape between A-10 and W-10.

3.4. Linear shrinkage

In terms of different powder-mixing methods, the linear shrinkage of sample A-10 decreased slightly from 14.6% to 13.7% while the linear shrinkage of sample W-10 increased to 15.4% compared to the sample without PVP addition, as shown in Table 1. Combined with the SEM results, it seems that both porosity and pore shape can affect the linear shrinkage. Sample W-10 with uniform small pores exhibits the highest linear shrinkage (15.4%) whereas sample A-10 with porous channels experiences the lowest linear shrinkage (13.7%). This is presumably because the formation and alignment of porous channels reduces the linear shrinkage along the length of bar-shaped samples. The sample without porous channels shrinks more evenly in all directions, resulting in a greater linear sintering shrinkage (W-10).

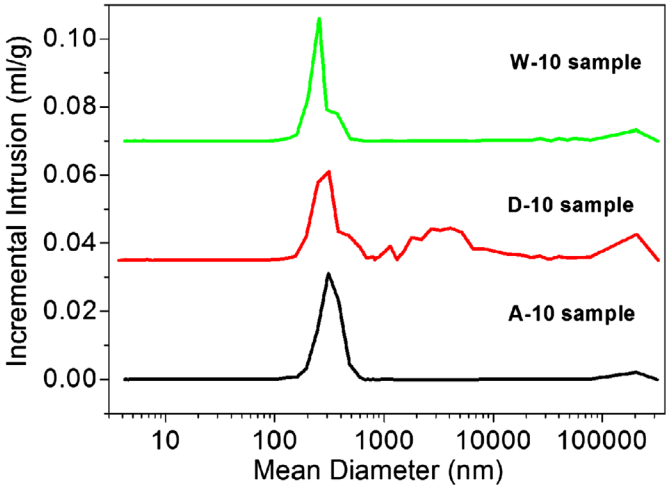

Fig. 3. Pore size distribution of sintered samples.

For the samples prepared with the acetone-mixing method, the linear shrinkage is almost unchanged when the amount of PVP increases from 5 wt% to 10 wt%; and decreases slightly from 13.7% to 12.8% as the amount of PVP increases to 20 wt%. This is likely due to more porous channels formed in A-20 sample.

3.5. Mechanical properties

The mechanical strength of all samples is summarized in Table 2. Among the samples prepared via different powder-mixing methods, sample A-10 has the highest bending strength, 140.2 MPa and sample D-10 has the lowest bending

strength, only 43.4 MPa. In sample D-10, large pores created by raw PVP powder are the main reason for the highest porosity and thus lowest mechanical strength. Although sample W-10 has more uniform pore structure and continuous solid phase than A-10, the bending strength of the former is approximately 28 MPa lower than that of the latter. The difference in bending strength can be attributed to their pore shapes.

Brown et al. [16] studied the strength-porosity relation involving different pore geometries and orientations and concluded that geometrical effects were dominant in determining the strength, and the strength-porosity relation could be expressed as

$$\sigma = \sigma_{max} A_{\text{solid}} / A_{\text{total}} \quad (1)$$

or

$$\sigma = \sigma_{\max}[1-\sum_i(\alpha_i p_i)] \quad (2)$$

$$\alpha_i = x_i A_i / v_i \quad (3)$$

where A_{solid} is defined as the total effective solid area that lies in a plane normal to the stress (a minimum load-bearing area or minimum solid contact area, and it does not lie in a plane normal to the stress but in an irregular surface, the fracture surface); A_{total} is the total cross-section area and $\sigma_{\max}$ is the strength of the sample when the porosity is 0 ($p=0$). In Eqs. (2) and (3), the subscript i indicates the ith type of pores; p_i is the porosity of the ith type of pores; x_i is a characteristic length of the ith type of pore, A_i is the projected maximum cross-sectional area of the ith type of pore and v_i is the volume of a single pore of the ith kind. Thus, α_i is a factor that closely related to pore morphology.

It can be seen from Eq. (2) that at a similar porosity a_i is the dominant factor in determining the strength of final products. According to the values of α_i with different pore shape and orientation calculated by Brown, for cylindrical pores, α_i is 1.00 if the axis of pores is parallel to applied tensile stress and 1.27 if the axis of pores is normal to the stress; α_i for spherical pores is 1.5. Therefore, at a similar porosity, porous materials with cylindrical pores have higher minimum load-bearing area or minimum solid contact area, thus higher strength than those with spherical pores in terms of comparable porosity.

As observed with SEM, there exist many pores connected together and some aligned long cylindrical pores in A-10, and these unique porous channels increase the minimum solid contact area, thus having higher bending strength as compared with the W-10 sample. The Young's modulus shows a similar trend among these samples. Sample A-10 has the highest value (57.4 GPa), which is slightly higher than that of sample W-10 (53.9 GPa) and is about 4.4 times higher than that of sample D-10 (10.7 GPa). The elastic properties of porous ceramics, such as Young's modulus, are proportional to the minimum solid contact area between the ceramic particles [17,18]. Similar to the strength–porosity relation, Young's modulus decreases with increasing the porosity [19,20]. Sample D-10 has the highest porosity and consequently the lowest Young's modulus. For samples A-10 and W-10, the difference in pore morphology leads to the difference in solid contact area, thus resulting in the difference in elastic properties.

Among the samples prepared using the acetone-mixing method, an increase in the amount of PVP from 0 wt% to 10 wt% leads to an increase in the bending strength from 52.2 MPa to 140.2 MPa, and then a decrease to 77.0 MPa as the content of PVP increased to 20 wt%. A similar trend is observed in Young's modulus. The addition of 10 wt% PVP in the alumina increases the Young's modulus by a factor of 3.5, i.e., from 12.91 GPa to 57.36 GPa. However, the Young's modulus decreases slightly to 50.65 GPa when the PVP amount further increases to 20 wt%. In the dry pressing of PVP–alumina powder prepared using acetone as solvent, uniformly dispersed PVP particles with large particle sizes tend to move easily and stick together to form aligned "PVP fibers" in the ceramic green bodies, and such a process also brings alumina particles closer to each other. This can promote neck growth between touching particles, and formation of aligned porous channels in the sintering process, thus increasing the bending strength. In addition, with increasing the amount of PVP from 10 wt% to 20 wt%, the average grain size of the sample decreases from 1.2 μm to 0.7 μm; whereas the average grain size of the sample prepared without PVP is 1.5 μm (Table 2). This clearly indicates that the addition of PVP leads to a decrease in grain growth. Since both A-0 and A-10 have a similar porosity, the smaller grain size of A-10 should explain its higher mechanical strength as it is generally accepted that the strength is inversely proportional to the grain size at the similar porosity [21]. The reason that A-20 exhibits lower strength than A-10 is that the former has higher porosity than the latter.

The strength of samples prepared in our work is also compared to that of samples with a similar porosity reported in the literature, as listed in Table 3. From Table 3, it can be seen that the strength of samples prepared in our work with PVP addition is relatively higher compared to that of samples reported in the literature. The high strength might be due to the fact that PVP particles can "squeeze" alumina particles, which on one hand makes alumina particles closer, thus improving neck growth during sintering, and on the other hand limits the grain growth.

In the porous alumina samples prepared from the same batch of powder via dry pressing, the variation in the microstructure is presumably greater than that in the overall porosity and

Table 2
Mechanical properties, average grain size and standard deviation value of samples.

Sample	Porosity (%)	Average grain size (μm)	Bending strength (MPa)	Standard deviation values of bending strength (MPa)	Young's modulus (GPa)
A-10	31.3	1.2	140.2	21.4	57.4
W-10	30.2	–	111.8	13.8	53.9
D-10	43.5	1.2	43.4	12.1	10.7
A-0	32.0	1.5	52.2	12.3	12.9
A-5	33.8	1.3	127.8	17.0	40.3
A-20	40.9	0.7	77.0	18.5	50.7

Table 3
Strength of porous alumina made in this paper and references.

References	Porosity range (%)	Strength (MPa)	Consolidation method
Alumina made in this work without PVP addition*	30	52.2	Pressureless sintering
Alumina made in this work with PVP addition**	30–40	77–140	Pressureless sintering
Ref. [21]	25–40	40–150	Hot pressing
Ref. [10]	28	74	Pressureless sintering
Ref. [22]	35–40	35–52	Pressureless sintering

*Sample A-0.
**Sample A-5, A-10, A-20.

average pore size. This may explain large standard variations in their mechanical properties (Table 2) In particular, sample A-10 has the highest strength, but its standard deviation is high too ($s=21.4$) due to the variation in the alignment of cylindrical porous channels. The bending strength of A-10 sample was in the range of 110–164 MPa, with a difference of 54 MPa. By contrast the difference between the maximum and minimum strength values is 33 MPa and 32 MPa for D-10 and W-10, respectively; both D-10 and W-10 have low deviation values (12.1 and 13.7, respectively).

4. Conclusions

(1) Porous alumina ceramics with porosity of 30%–45% were made with PVP as a pore-former and binder.
(2) Different solubility of PVP in acetone and water led to different dispersion of PVP in alumina and final porous structure. The use of water resulted in a more uniform pore structure compared to acetone assisted ball milling and dry milling.
(3) Acetone-mixing PVP/alumina sample had the highest strength as well as Young's modulus due to formation of cylindrical pore structure. Both porosity and pore morphology affected mechanical properties; the samples with cylindrical pores had the highest bending strength as well as Young's modulus as compared with those prepared without PVP at a similar porosity. Higher bending strength was obtained for the acetone-mixing alumina sample, and the deviation value of strength was also higher compared to the water-mixing alumina sample.
(4) The uniform dispersion of PVP was effective in limiting grain growth during sintering, and greater grain bonding strength and solid contact area could be achieved, thus increasing the toughness of porous alumina ceramics.

Acknowledgments

The authors acknowledge the financial support of the National Center of Excellence in Desalination Australia which is funded by the Australian Government through the Water for the Future initiative. H.W. thanks the Australian Research Council for a Future Fellowship.

References

[1] I.Y. Guzman, Certain principles of formation of porous ceramic structures. Properties and applications (a review), Glass and Ceramics 60 (2003) 280–283.
[2] F. Patel, M.A. Baig, T. Laoui, Processing of porous alumina substrate for multilayered ceramic filter, Desalination and Water Treatment 35 (2011) 33–38.
[3] F.Q. Tang, H. Fudouzi, T. Uchikoshi, Y. Sakka, Preparation of porous materials with controlled pore size and porosity, Journal of the European Ceramic Society 24 (2004) 341–344.
[4] T.S. Kim, I.C. Kang, T. Goto, B.T. Lee, Fabrication of continuously porous alumina body by fibrous monolithic and sintering process, Materials Transactions 44 (2003) 1851–1856.
[5] S. Baklouti, T. Chartier, J.F. Baumard, Mechanical properties of dry-pressed ceramic green products: the effect of the binder, Journal of the American Ceramic Society 80 (1997) 1992–1996.
[6] S. Baklouti, T. Chartier, C. Gault, J.F. Baumard, Young's modulus of dry-pressed ceramics: the effect of the binder, Journal of the European Ceramic Society 19 (1999) 1569–1574.
[7] Z.Y. Deng, T. Fukasawa, M. Ando, G.J. Zhang, T. Ohji, High-surface-area alumina ceramics fabricated by the decomposition of $Al(OH)_3$, Journal of the American Ceramic Society 84 (2001) 485–491.
[8] E. Gregorova, W. Pabst, Process control and optimized preparation of porous alumina ceramics by starch consolidation casting, Journal of the European Ceramic Society 31 (2011) 2073–2081.
[9] R.M. Khattab, M.M.S. Wahsh, N.M. Khalil, Preparation and characterization of porous alumina ceramics through starch consolidation casting technique, Ceramics International 38 (2012) 4723–4728.
[10] E.M. Tomilina, O.V. Pronina, E.S. Lukin, G.G. Kagramanov, Porous alumina-based ceramic, Glass and Ceramics 57 (2000) 210–211.
[11] R.L. Menchavez, L.-A.S. Intong, Red clay-based porous ceramic with pores created by yeast-based foaming technique, Journal of Materials Science 45 (2010) 6511–6520.
[12] Y.-W. Moon, K.-H. Shin, Y.-H. Koh, W.-Y. Choi, H.-E. Kim, Porous alumina ceramics with highly aligned pores by heat-treating extruded alumina/camphene body at temperature near its solidification point, Journal of the European Ceramic Society 32 (2012) 1029–1034.
[13] S.M. Liu, K. Li, R. Hughes, Preparation of porous aluminium oxide (Al_2O_3) hollow fibre membranes by a combined phase-inversion and sintering method, Ceramics International 29 (2003) 875–881.
[14] B.F.K. Kingsbury, K. Li, A morphological study of ceramic hollow fibre membranes, Journal of Membrane Science 328 (2009) 134–140.
[15] J.C. Wurst, J.A. Nelson, Lineal intercept technique for measuring grain size in two-phase polycrystalline ceramics, Journal of the American Ceramic Society 55 (1972) 109–111.
[16] S.D. Brown, R.B. Biddulph, P.D. Wilcox, A strength-porosity relation involving different pore geometry and orientation, Journal of the American Ceramic Society 47 (1964) 320–322.
[17] R.W. Rice, Comparison of stress-concentration versus minimum solid area based mechanical property porosity relations, Journal of Materials Science 28 (1993) 2187–2190.

[18] R.W. Rice, Evaluation and extension of physical property-porosity models based on minimum solid area, Journal of Materials Science 31 (1996) 102–118.

[19] A.K. Mukhopadhyay, K.K. Phani, An analysis of microstructural parameters in the minimum contact area model for ultrasonic velocity–porosity relations, Journal of the European Ceramic Society 20 (2000) 29–38.

[20] F.P. Knudsen, Dependence of mechanical strength of brittle polycrystalline specimens on porosity and grain size, Journal of the American Ceramic Society 42 (1959) 376–387.

[21] T. Ostrowski, J. Rodel, Evolution of mechanical properties of porous alumina during free sintering and hot pressing, Journal of the American Ceramic Society 82 (1999) 3080–3086.

[22] A. Kritikaki, A. Tsetsekou, Fabrication of porous alumina ceramics from powder mixtures with sol–gel derived nanometer alumina: effect of the mixing method, Journal of the European Ceramic Society 29 (2009) 1603–1611.